

ORIGINAL

## Optimization of the Design of a Centrifugal Pump of the Automotive Engine Cooling System

### Optimización del diseño de una bomba centrífuga del sistema de refrigeración del motor automotriz

Edilberto Antonio Llanes-Cedeño<sup>1</sup>  , Édison Argüello Maya<sup>2</sup> , Juan Carlos Quinchuela Paucar<sup>3</sup> , Rodrigo Rigoberto Moreno-Pallares<sup>3</sup> , Lenin Montalvo Ochoa<sup>4</sup> 

<sup>1</sup>Universidad Internacional SEK, Department of Mechanics. Quito, Ecuador.

<sup>2</sup>Universidad de las Fuerzas Armadas ESPE, Departamento de Ciencias de la Energía y Mecánica Sede Latacunga. Av. General Rumiñahui S/N.

<sup>3</sup>Escuela Superior Politécnica de Chimborazo (ESPOCH), Faculty of Mechanics. Riobamba, Ecuador.

<sup>4</sup>Lundingold, Maintenance senior planner. Quito, Ecuador.

**Cite as:** Llanes-Cedeño EA, Argüello Maya Édison, Quinchuela Paucar JC, Moreno-Pallares RR, Montalvo Ochoa L. Optimization of the Design of a Centrifugal Pump of the Automotive Engine Cooling System. Salud, Ciencia y Tecnología. 2025; 5:2514. <https://doi.org/10.56294/saludcyt20262514>

Submitted: 09-08-2025

Revised: 12-10-2025

Accepted: 10-12-2025

Published: 11-12-2025

Editor: Prof. Dr. William Castillo-González 

Corresponding Author: Edilberto Antonio Llanes-Cedeño 

#### ABSTRACT

**Introduction:** the study focused on analyzing the design of a centrifugal pump in vehicle engine cooling systems. Cavitation, a phenomenon that impacts the efficiency and durability of hydraulic components, was examined as a key variable. Based on the geometry of the centrifugal pump impeller, computational fluid dynamics (CFD) simulations and experimental validation were employed.

**Method:** three combined strategies were implemented: analysis of hydraulic parameters using equations; precise modeling of flow behavior to evaluate geometric configurations; and comparison of numerical data with actual pressure and flow measurements. Fluctuations in the motor diameter (61 mm, 62 mm, and 63 mm) were analyzed under normal operating conditions and acceleration.

**Results:** increasing the inlet diameter to 61 mm proved to be the ideal solution, achieving a 5 % increase in pump inlet pressure and significantly reducing the risk of cavitation. CFD methods were confirmed as valuable tools for refining designs, demonstrating a high correlation with experimental data.

**Conclusions:** the effective use of tools such as CFD to address critical challenges in automotive engineering is emphasized, optimizing both technical performance and environmental impact. Furthermore, it increases hydraulic efficiency and reduces cavitation in centrifugal pump in vehicle engine cooling systems.

**Keywords:** Centrifugal Pump; Geometrical Parameters; Volute Design; Engine Automotive; Computational Fluid Dynamics (CFD).

#### RESUMEN

**Introducción:** el estudio se centró en el análisis del diseño de una bomba centrífuga para sistemas de refrigeración de motores de vehículos. Se examinó la cavitación, un fenómeno que afecta la eficiencia y la durabilidad de los componentes hidráulicos, como una variable clave. A partir de la geometría del impulsor de la bomba centrífuga, se emplearon simulaciones de dinámica de fluidos computacional (CFD) y validación experimental.

**Método:** se implementaron tres estrategias combinadas: análisis de parámetros hidráulicos mediante ecuaciones; modelado preciso del comportamiento del flujo para evaluar configuraciones geométricas; y comparación de datos numéricos con mediciones reales de presión y caudal. Se analizaron las fluctuaciones en el diámetro del motor (61 mm, 62 mm y 63 mm) en condiciones normales de funcionamiento y durante la aceleración.

**Resultados:** aumentar el diámetro de entrada a 61 mm resultó ser la solución ideal, logrando un incremento del 5 % en la presión de entrada de la bomba y reduciendo significativamente el riesgo de cavitación. Los métodos de CFD se confirmaron como herramientas valiosas para el perfeccionamiento de los diseños, demostrando una alta correlación con los datos experimentales.

**Conclusiones:** se destaca el uso eficaz de herramientas como la CFD para abordar desafíos críticos en la ingeniería automotriz, optimizando tanto el rendimiento técnico como el impacto ambiental. Además, incrementa la eficiencia hidráulica y reduce la cavitación en las bombas centrífugas de los sistemas de refrigeración de motores de vehículos.

**Palabras clave:** Bomba Centrífuga; Parámetros Geométricos; Diseño de Voluta; Motor de Automóvil; Dinámica de Fluidos Computacional (CFD).

## INTRODUCTION

The internal combustion engine (ICE) has been constantly analyzed with the aim of reducing CO<sub>2</sub> and harmful gas emissions while simultaneously improving mechanical efficiency.<sup>(1)</sup> Work is underway to optimize ICE technology, providing considerable room for progress. Within these optimization fields, reducing engine size<sup>(2)</sup> and using biofuels are fundamental technological paths.<sup>(3,4)</sup> Furthermore, engine thermal management is a relevant field of intervention that shows an optimal balance between the reduction of CO<sub>2</sub> and cost increase.<sup>(5)</sup>

### Evolution of centrifugal engine pump design

One of the most significant complications involved in the operation of a centrifugal pump in the heat engine of a vehicle or an automotive machine is the wide range of load and rpm values in which it operates.<sup>(6)</sup> Therefore, the centrifugal pump must be designed to maintain adequate operating conditions within the range of revolutions per minute (rpm) at which an automotive machine's engine typically operates. However, if the pump operates at a low revolution speed, providing limited flow rates and heads, the pump efficiency presents figures of 15-20 % or even lower.<sup>(7)</sup> Furthermore, analyzing the engine operating height above 2700 meters above sea level will propose a higher operating load.<sup>(8,9,10,11)</sup>

### Advances in optimization techniques

According to Shah et al.<sup>(12)</sup>, the application of CFD in the design of pumps and turbines began about 30 years ago. The first steps coincided with introducing the finite element method in CFD and have been characterized by simplified solutions of quasi-3D Euler equations and full 3D flow. Over the years, the complexity has been increasing through three-dimensional Euler equations and simulations through the Reynolds Averaged Navier - Stokes (RANS) equations of simple blades using finite volume methods, extending to simulations of complete machines. CFD analysis is widely used but has a high computational cost. The internal forces of a variable displacement pump can be evaluated, and it was found that the effect of pump speed on the internal force is greater than that of pump eccentricity.<sup>(13)</sup>

In the literature, numerous works have focused on improving the shape of centrifugal pumps,<sup>(14,15,16)</sup> although their most significant focus is on a single component, such as the impeller, diffuser or volute. Furthermore, the geometric parameterization is simple, and the thickness distribution has not been considered. Despite the extensive literature in the area of optimization for wind and gas turbines and aerofoils, robust design, at least as far as is known.<sup>(17)</sup>

### The role of computational fluid dynamics

According to Mentzos et al.<sup>(9)</sup>, the complex internal flow in a centrifugal pump is not yet altogether understood. However, computational fluid dynamics (CFD) can predict it quite well. Therefore, this is a key tool for designers. According to Hedi et al.<sup>(10)</sup>, centrifugal pumps have a wide application in the field of engineering. Thus, the pumping system must operate in special applications over various conditions. Therefore, knowledge of pump performance under different operating conditions is a necessity. Furthermore, according to Bacharoudis et al.<sup>(11)</sup>, the complexity of flow in a turbomachine is largely due to the three-dimensional structures developed involving turbulence, secondary flows, instability, etc. At the impeller outlet, circumferential distortion appears in the internal flow due to the asymmetric characteristics of the spiral and the tongue. In addition, the impeller-volute interaction causes dynamic effects that influence the pump's performance. Non-uniform flow conditions and pressure fields generate unbalanced radial forces in the pump.

Therefore, the general objective of this research was to analyze the design of a centrifugal pump for internal combustion engine cooling systems, based on the geometry of the centrifugal pump impeller, computational fluid dynamics (CFD) simulations and experimental validation, to evaluate its efficiency.

## METHOD

This work addresses a quantitative investigation where pressure, flow and performance parameters are determined as a function of the variation of the impeller diameter, applying the empirical scientific methods (experimentation: by varying the diameter of the impeller and observing how the other dependent variables vary), and the mathematical and simulation method.

## Variables, Data Collection, and Processing

The cavitation phenomenon depends on two factors: the pump installation and the pump itself. The most important part of the centrifugal pump that defines its operating characteristics is the impeller, since its geometry, along with the rotational speed, determines the pressure and flow rate. The variable analyzed in this research is the inlet diameter, or diameter at the base of the vanes, whose original dimension is 60 mm. The proposed redesign involves increasing this diameter. Three additional studies are conducted: in the first case, the diameter is increased to 61 mm; in the second, to 62 mm; and in the last, to 63 mm. All these results are compared to present an evaluation of the hydraulic performance and the pressures that directly and significantly influence the cavitation of the system.

## Experimental Data

The values will be determined under the machine's real operating conditions: pressure, flow rate, and operating temperature. These values will be recorded for the different operating regimes of the centrifugal pump.

The application requires compliance with certain conditions to ensure test results: Test prototype, test environment, measuring instruments, and test conditions. Once these conditions have been met, the tests will be performed, and the data will be collected.

## Analytical modeling

The project involved the analysis of the fluid and its dimensions in the centrifugal pump of the engine cooling system. The input values, such as flow rate, pressure, height difference, angular speed of the impeller, and geometry of the blades, were included. The flow and pressure values for the study have been obtained through the experimental method, and geometric values have been obtained through CAD modeling, see figure 1, due to their complementarity at this point.

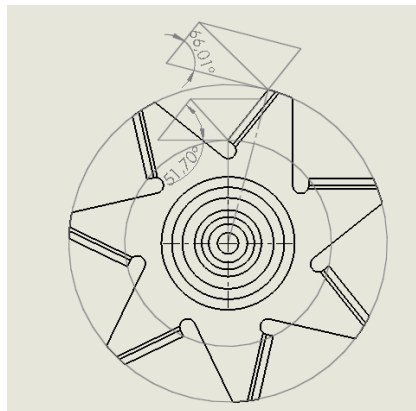


Figure 1. Impeller's analysis in the entry and exit angles

The theoretical analysis was carried out on the geometry of the centrifugal pump impeller, where the speed triangles in Figure 1 and their magnitudes are analyzed<sup>(18)</sup>; these values are directly related to the angular speed of the centrifugal pump impeller, the tests were carried out in the two main operating regimes: in idle regime 1077,9 rpm and nominal regime 2627,65 rpm. Regarding the main dimensions obtained dimensionally in the impeller,  $D_1 = 0,060$  m,  $D_2 = 0,090$  m,  $b = 0,018$  m,  $B_1 = 51,7^\circ$ ,  $B_2 = 66,01^\circ$ . The values of the main vectors were obtained by applying the equations of the velocity triangles. In this case, the velocity equation was used at the entrance of the blades, and equation (1) is the same for the exit of the blades.<sup>(19)</sup>

$$C_{1u} = U_1 - C_{1m} / (\tan B_1) \quad (1)$$

It is considered taking into account the volumetric flow rate equations, equations (2) and (3):<sup>(20)</sup>

$$Q = A_v \quad (2)$$

$$Q = \pi D_1 b_1 C_{1m} \quad (3)$$

The continuity equation, equation (4), helps to relate the entry triangle and the exit triangle.

$$C_{2m} = (b_1 D_1) / (b_2 D_2) C_{1m} \quad (4)$$

Where  $b_1$  represents the height of the blades at the inlet. In this study, the thickness of the blades along the impeller is constant, so  $b_1 = b_2$ . Then, according to equation (5), the value of the theoretical head or Euler head delivered by the pump is obtained.<sup>(21)</sup>

$$H_u = \pm (U_1 C_{1u} - U_2 C_{2u}) / g \quad (5)$$

These data must be validated and compared with the values obtained through equation (6), the first expression of the valuable height.<sup>(22)</sup>

$$H = (P_s - P_e) / \rho g + z_s - z_e + (V_s^2 - V_e^2) / 2g \quad (6)$$

Then equation (7) is applied, practical or effective head of the pump.

$$H = H_u - H_{r-1nt} \quad (7)$$

The pump's hydraulic performance can be found by applying equation (8), where  $H_{r-1nt}$  represents the system's losses and the eventual difference between the analytical and experimental methods.<sup>(23)</sup> research on improving the hydraulic performance of the pump as turbine (PAT).

$$\eta_h = H / H_u \quad (8)$$

The CFD method requires information about the type of flow that governs the centrifugal pump to apply the most appropriate numerical solution conditions and thereby determine the type of flow that the Reynolds number should find, equation (9).<sup>(24)</sup>

$$Re = DV / v \quad (9)$$

### CFD variables modeling

The application of the CFD method requires a computational tool and at least one software program that incorporates the CAD module and the CFD module in its internal code. According to Xamán<sup>(25)</sup>, the CFD procedure is divided into the following parts: pre-processing, solver, and post-processing.

Pre-processing.- It constitutes the first part of the procedure. It consists of entering data into the software, creating the computational geometric domain or domains, and generating the computational mesh. It was subdivided into the following stages:

Define geometry or computational domain.- This aspect digitizes the physical information of the geometry of the centrifugal pump and all its components. The software was used in its modeling, see figure 2 and 3. The geometric precision between the genuine and digital parts is crucial since their discrepancy generates uncertainty problems in the computational simulation results.<sup>(25)</sup> Physical data for digitization was collected with precision instruments; the digital model has been validated by printing the digital geometry at full scale and comparing this paper with the fundamental part.

Before the meshing procedure, there is an important consideration regarding the geometric parts; the CFD software analyzes the fluid volumes, that is, the volume of fluid that circulates in the centrifugal pump. Therefore, performing the operations required to find said volumes before entering information into the CFD module is necessary. First, the procedure was carried out to extract the domain volume of the fluid in the volute. In the fluid domain of the volute, inlet and outlet volumes are also considered. This improves the influence circuit of the centrifugal pump in the simulation, which aims to obtain more developed and actual flows in the simulation. Then, the same domain location procedure was performed for the impeller, where the volume with which the impeller directly interacts was extracted from the volume of the impeller; the result will be known as the influence volume of the impeller, see figure 4.

To conclude, the volumes of the fluid domain were assembled, see figure 5. At this point, it is taken into consideration that in addition to the movement of the fluid through the impeller and the volute, there is the movement of the impeller. In an adequate analysis process<sup>(26)</sup>, the two movements must be taken into account, so the multiple references option of the CFD computational tool was used to simulate this condition. This model is a quasi-stable state. Approximation in which areas of the mesh cells move at different rotational speeds.

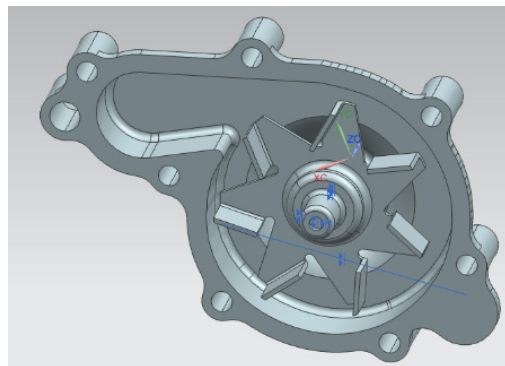


Figure 2. Volute and impeller modeling

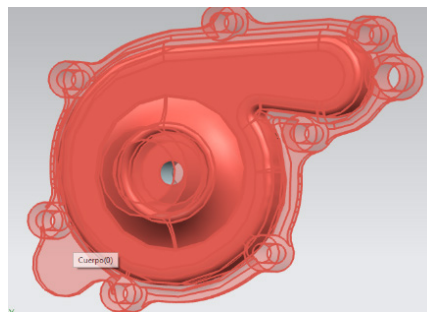


Figure 3. Casing working volume

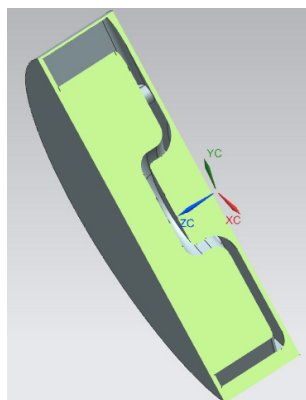


Figure 4. Impeller domain

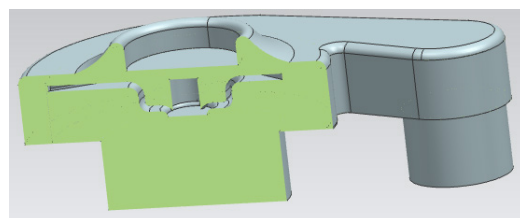


Figure 5. Fixed domain and mobile domain assembled

Numerical mesh generation.- Since the simulation procedure is carried out in the CFD module of the ANSYS 2023R2 software, prior to the meshing procedure, the domain solid must be exported. The two fluid domains (volute and impeller) are differentiated in the Mesh module, where the meshing of the part is carried out.

The meshing procedure is the procedure through which the flow influence volume is discretized into a finite number of volumes (MVF), also known as cells, each representing a node that is analyzed independently in the solution stage. Then, the results were added to obtain the total solution for the system. Still, in exchange, there will be a greater consumption of resources and computational time, and a finer mesh does not always represent a better solution.<sup>(25)</sup>

Tetrahedral meshing has been used in the influence volumes with finer meshes in areas of closed radii,<sup>(27)</sup>

impeller influence zones and sharp geometries, and coarser mesh size in volumetric zones with larger volume geometries of less sharpness see figure 6. That was done to optimize the computational resource, making more precise calculation zones where more considerable pressure and velocity gradients are expected and saving computational resources in areas with less change in gradients.

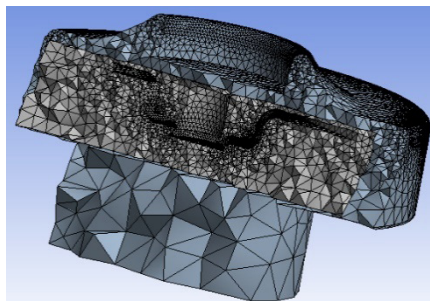


Figure 6. Exportation

Figure 7 shows the mesh sizes used, and the number of nodes obtained in the process for the volute's domain of influence, and figure 8 shows the volume of the impeller domain.

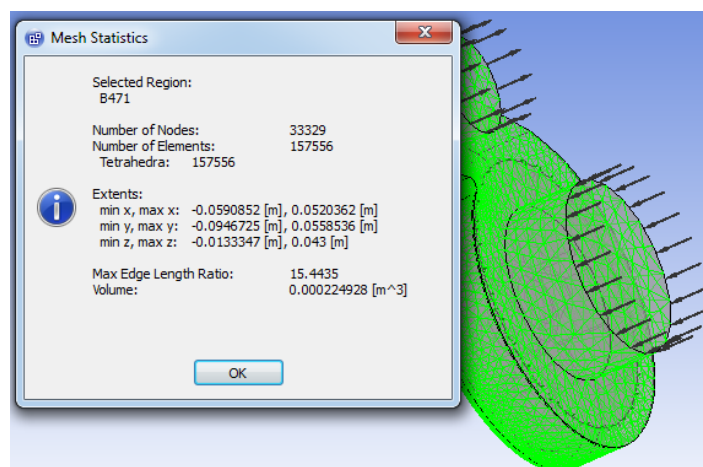


Figure 7. Meshing, Meshing statistics on volute control volume

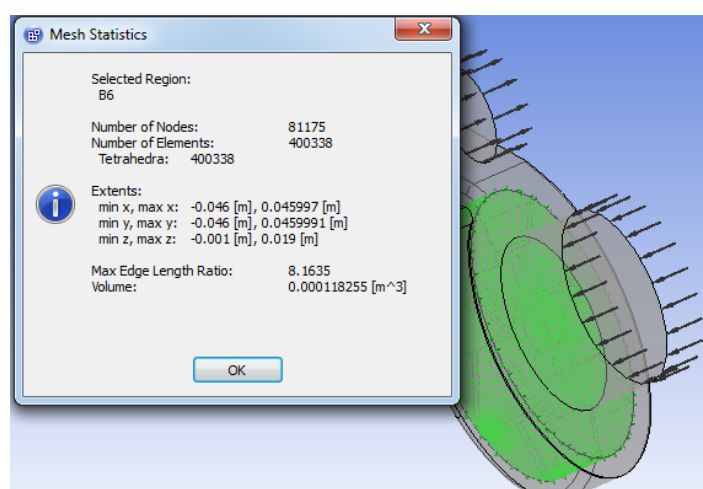


Figure 8. Meshing, Meshing statistics in impeller control domain volume

The physical phenomenon that was simulated is the behavior of the fluid passing through the control domains of the impeller and the volute of the element under study through CFD. In contrast, the impeller communicates energy to the flow.<sup>(28)</sup> According to the geometric and physical characteristics of the element, the flow in the volume of the impeller domain is radial, with the axial flow equal to zero. At the same time, the velocity in the

intake is axial. Finally, the flow type is considered turbulent according to the results obtained in the analytical method.

Taking these considerations into account, the physical values that represent the boundary values and that are applied are:

Impeller revolutions: the impeller speed is proportional to the crankshaft speed, and it has been measured, and then computed with an average value of 2627,7 rpm at nominal speed.

Fluid: those considered in the study will be water instead of the coolant; its physical-chemical characteristics are available in the software, see figure 9. The numerical calculations consider the characteristics of water at the engine operating temperature, and the case is 85 °C, as well as the atmospheric pressure of Quito.

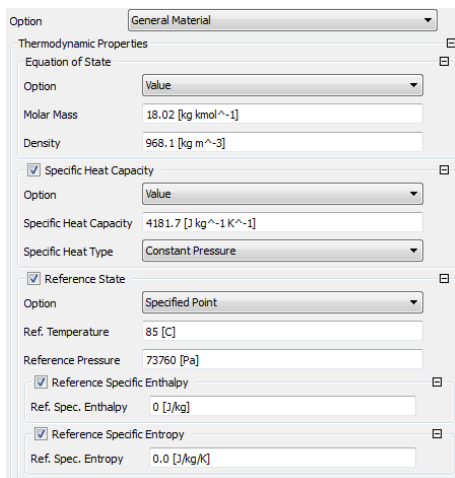


Figure 9. Fluid properties

Temperature: the average operating temperature of an engine is 85 °C.<sup>(29)</sup> Flow rate: The nominal operating regime whose value is 1,31 kg/s, see figure 10.

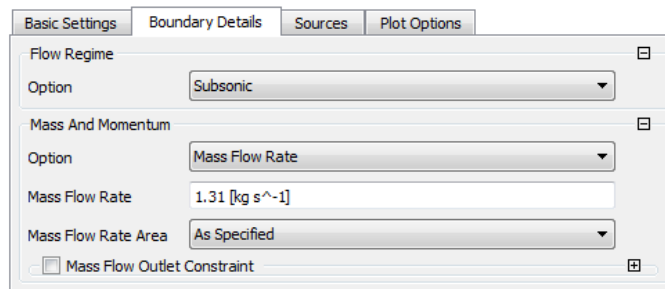


Figure 10. Centrifugal pump mass flow

Inlet speed: According to equation 2, the pump's flow inlet speed in the motor's nominal operating regime is shown in figure 11.

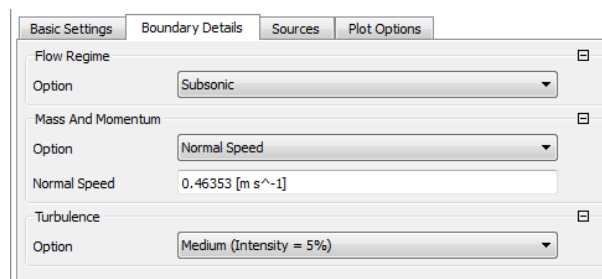


Figure 11. Normal speed at the pump inlet

The boundary conditions: Three boundaries are selected: entry, exit, and wall or solid. Figure 12 shows the entry with arrows towards the interior of the control volume. The case is analogous to the exit, which is distinguished by being formed by a green mesh<sup>(12)</sup> and the physical reality.<sup>(30)</sup>

In the internal boundary conditions, in the case of the simulation of a centrifugal pump, within the computational domain in the rotor, an energy exchange occurs that dramatically changes the nature of the flow, increasing energy that was physically translated into flow and pressure. This internal boundary condition is achieved with the previous step of differentiating the control volumes into stationary and rotating, and then in the CFD module, including an interface that communicates the two volumes and an internal rotary mesh.<sup>(24)</sup>

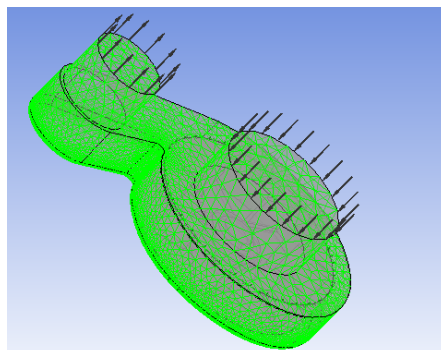


Figure 12. Entering geometric constraints

Under the conditions of numerical calculation or CFD: taking as reference analogous study procedures, such as the work of Bacharoudis et al.<sup>(11)</sup> The following considerations are taken in the software: the calculations are executed with the Ansys CFX module that uses the finite volume method (MVF) for the solutions of stable NAVIER-STOKES equations of incompressible fluids<sup>(31)</sup>, according to the analysis it is determined that the type of flow in the centrifugal pump is turbulent, therefore in addition to the transport and conservation equations, an algorithm must be applied that simulates turbulent flow, for the present case the turbulence is modeled with the standard k- $\epsilon$  model, given that its results have been very acceptable for the majority of cases in which fluid turbulence intervenes.

The number of iterations depends on the chosen convergence criterion, which in turn depends on the convergence of the numerical solution concerning the exact solution. According to Cengel<sup>(24)</sup> it was expected that for complicated problems with fine meshes, the residuals stabilize at values even higher than 10-3; therefore, in the present study, a value of 0,001 has been chosen in order to find a more precise solution in terms of the residual. Chosen convergence is the RMS, while the number of iterations has been set at 400, which means that the program will iterate until 400 iterations have been completed or until the remainder is less than 1E-3, see figure 13.

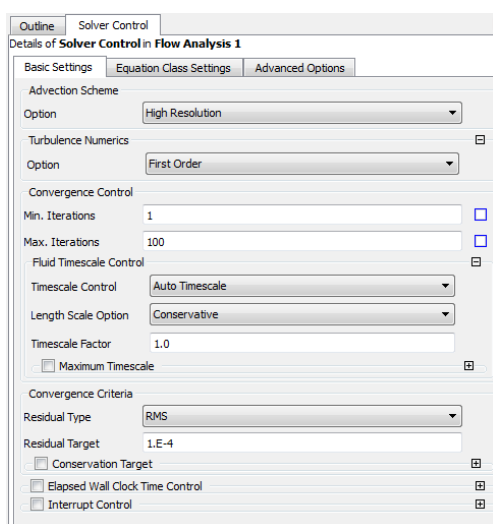


Figure 13. Entry of calculation conditions, iterations, and remainder

Finally, the solver module of the commercial software ANSYS was used for the numerical resolution of the steady-state NAVIER-STOKES equations. Likewise, in the numerical solution where the variables are analyzed, these results are interpreted, compared, validated, and serve as a reference for the design optimization procedure, which is the purpose of this study.

## RESULTS

### Experimental Results

In this case, an average value is taken for calculation, comparison and validation purposes.

$$P_s = 80,08260558 \text{ kPa}$$

This pressure value represents a gauge reading relative to atmospheric pressure. To obtain the total pressure, the two values must be added together: the previous value plus the atmospheric pressure value, which for the city of Quito is 73,760 kPa. Therefore:

$$P_s = 80,08260558 \text{ kPa} + 73,760 \text{ kPa}$$

$$P_s = 153,842 \text{ kPa}$$

### Flow rate test

Tables 1 and 2 present the average results of the five volume and flow rate measurements, under idle speed and nominal operating conditions. It can be observed that these parameters increase as the RPM increases.

Table 1. Flow tests in Idle regime

Average results Flow measurement			
Time (min)	rpm	Volume (L)	Water flow (L/s)
0	770	0	0
3	770	79,122	0,43956667

Table 2. Flow tests at nominal flow rate

Average flow measurement results			
Time (min)	rpm	Volume (L)	Water flow (L/s)
0	2176	0	0
3	2176	235,912	1,31062222

### Results of the analytical method

This section presents the analytical results obtained using equations (1) - (9), applied with the pressure and flow rate results obtained from the experimental method and the geometric values obtained in the CAD modeling process during the initial stage of the CFD method. Since the design of any mechanical component must be based on its most critical operating conditions to ensure the machine or part's design, this also guarantees proper functioning under more favorable conditions. Additionally, considering the desire to determine if cavitation conditions occur in the centrifugal pump during operation, and that these conditions are more likely to appear at high operating speeds<sup>(22)</sup>, the theoretical analysis will be performed at the nominal operating regime, which in this case is:

#### Nominal Regime: 2627,65 rpm

With this rotational speed and applying the speed triangles (see Figure 1), the following results are obtained:

#### Angular velocity

$$\omega = 275,16 \text{ rad/s}$$

#### Tangential velocities

$$u_1 = 8,255 \text{ m/s}$$

$$u_2 = 12,3822 \text{ m/s}$$

Flow rate: since the International System of Units (SI) is used, the average value found in table 2 is converted to  $\text{m}^3/\text{s}$ , obtaining:

$$Q = 1,3106 \times 10^{-4} \text{ m}^3/\text{s}$$

Applying equation (3) and solving for  $C_{1m}$ , we obtain:

$$C_{1m}=0,3863 \text{ m/s}$$

Applying equation (1) we obtain:

$$C_{1u}=7,95 \text{ m/s}$$

By the continuity equation (4)

$$C_{2m}=0,25753 \text{ m/s}$$

Applying equation (1) at the impeller outlet

$$C_{2u}=12,267 \text{ m/s}$$

Applying the theoretical head or Euler head equation (5) and taking into account a purely radial flow at the impeller inlet, we have:

$$H_u=15,48 \text{ m}$$

On the other hand, applying equation (6) between the inlet and outlet of the centrifugal pump, in the area where the pressure gauges have been mounted, figure (14), the useful height value of the pump is obtained.

$$H=8,69363 \text{ m}$$

Using equation (8) the hydraulic performance of the pump is obtained.

$$n_h=0,56$$

Power absorbed by the pump.

$$P=200 \text{ W}$$

Definition of flow type, according to equation (9), in nominal operating regime and at the inlet of the centrifugal pump, it is found that:

$$Re=0,46353 \times 0,06 / (1,005 \times 10^{-6})$$

$$Re=27673 > 2000$$

According to the result obtained, it is identified that the internal flow of the centrifugal pump is of the turbulent type, therefore, a method that simulates it must be applied in the CFD numerical solution.

## Pressure

Figure 14 shows the pressure graph in the pump's inlet and outlet areas. In the inlet area, the total pressure value is approximately 69060 Pa., while the experimental value obtained for the pressure reading in the same area is 69197,3 Pa. The pressure value in the pump's discharge is approximately 156100 Pa. in the CFD test, while in the experimental result, this value was 153842 Pa.

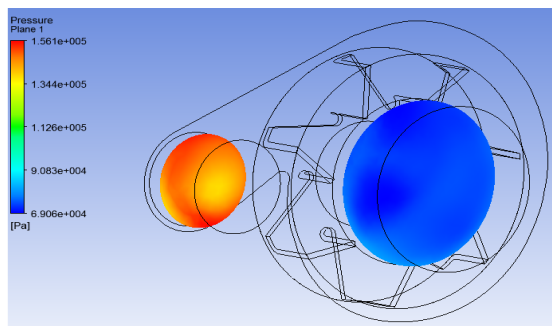


Figure 14. Pressure Graph

From a numerical point of view, the results are also very similar, considering that the difference between the results obtained in admission is 137 Pa. This result in terms of pressure is minimal, approximately 0,1 % of an atmosphere; additionally, the pressure graph obtained by CFD could be interpreted visually with an even greater approximation since the figure lends itself. However, it has not been considered convenient since it would result in a non-objective selection.<sup>(32)</sup>

On the other hand, the pressure results obtained in the pump's discharge zone are also close, with a maximum difference of 2258 Pa., representing a 1,5 % deviation between the two results. Thus, the numerical solution and the experimental results are considered convergent.

### Speed

The result of the simulation in terms of speed can be seen in figure 15; the speed is lower in the intake zone; according to logic, this shows that there is an exchange of energy between the impeller and the fluid, given that, the impeller causes an increase in the speed of the fluid, as can be seen in the area of influence of the impeller and volute. The speed decreases once the fluid leaves the volute area, becoming pressure according to the Bernoulli principle.<sup>(24)</sup>

$$A_1V_1 = A_2V_2$$

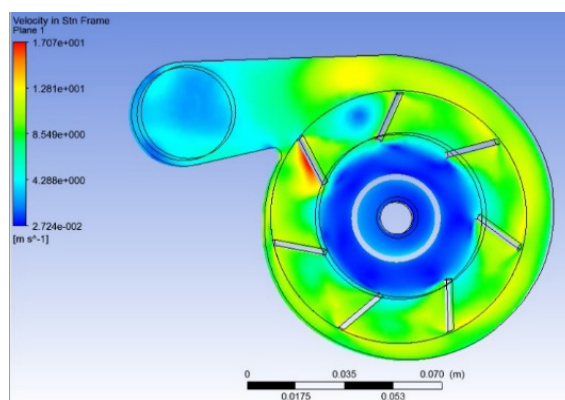


Figure 15. Speeds graph

### Cavitation

Cavitation is the phenomenon that occurs when, at any point in the flow, the pressure falls below the vapor pressure of the fluid at the operating temperature, producing the evaporation of the liquid in a bubble or cavity that later implodes causing cavitation, once the pressure rises sufficiently. Two phenomena occur in the cooling system pump: low inlet pressure and fluid temperature at approximately 85 °C under normal operating conditions.<sup>(29)</sup>

The experimental tests identified a peak of negative gauge pressure, or pressure below atmospheric pressure, during the engine's acceleration until its nominal speed, with a value of 11429 kPa. This value is a depression or a negative value concerning atmospheric pressure; the atmospheric pressure for the specific case of the study corresponds to the atmospheric pressure of Quito (2600 masl.) with a value of 73600 Pa., therefore, the pressure value in the inlet area of the pump at the moment of acceleration is:

$$73600 \text{ kPa} - 11429 \text{ kPa} = 62331 \text{ kPa}$$

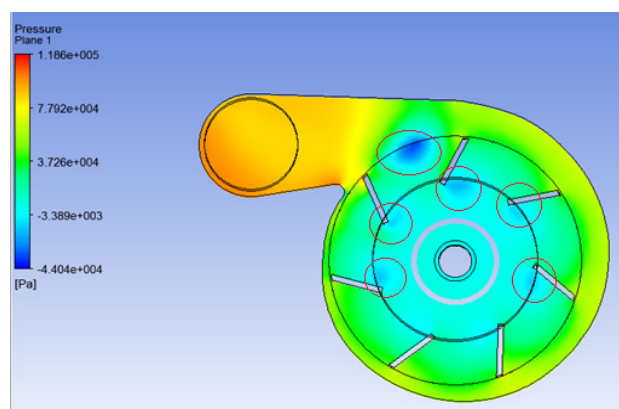


Figure 16. Low-pressure zones in the impeller

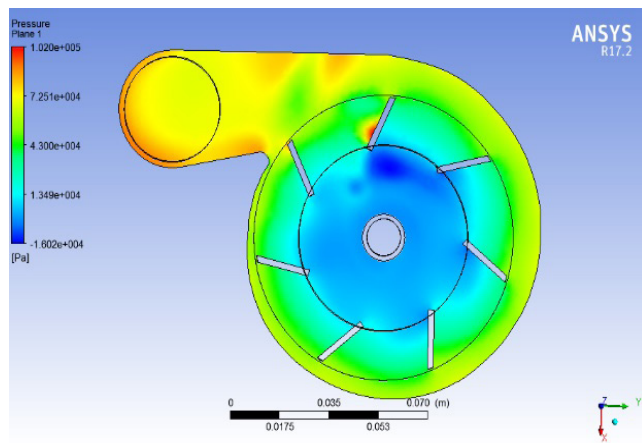


Figure 17. Engine acceleration moment pressures

This pressure value corresponds to the inlet of the centrifugal pump. Figure 16 has been obtained by simulating the real conditions during the engine acceleration process, in which, before engine acceleration, there is a low pressure at the pump outlet and a low flow rate. Taking into account that the normal operating temperature of the engine is 85 °C in the nominal regime and that this value can be increased during the machine's operation to values ranging from 95 °C, the physical conditions necessary for the cavitation phenomenon to occur are met and therefore it is demonstrated that the erosion phenomenon in the volute of the centrifugal pump was caused by cavitation<sup>(34)</sup>, due to the pressure variation as seen in figure 17.

According to the convergence criterion selected with a residue of 1E-4 and a maximum of 100 iterations monitoring the iteration process, in the case of the mass conservation equations, figure 18 shows that the residue stabilizes relatively from iteration No. 40 and remains stable until the process ends.

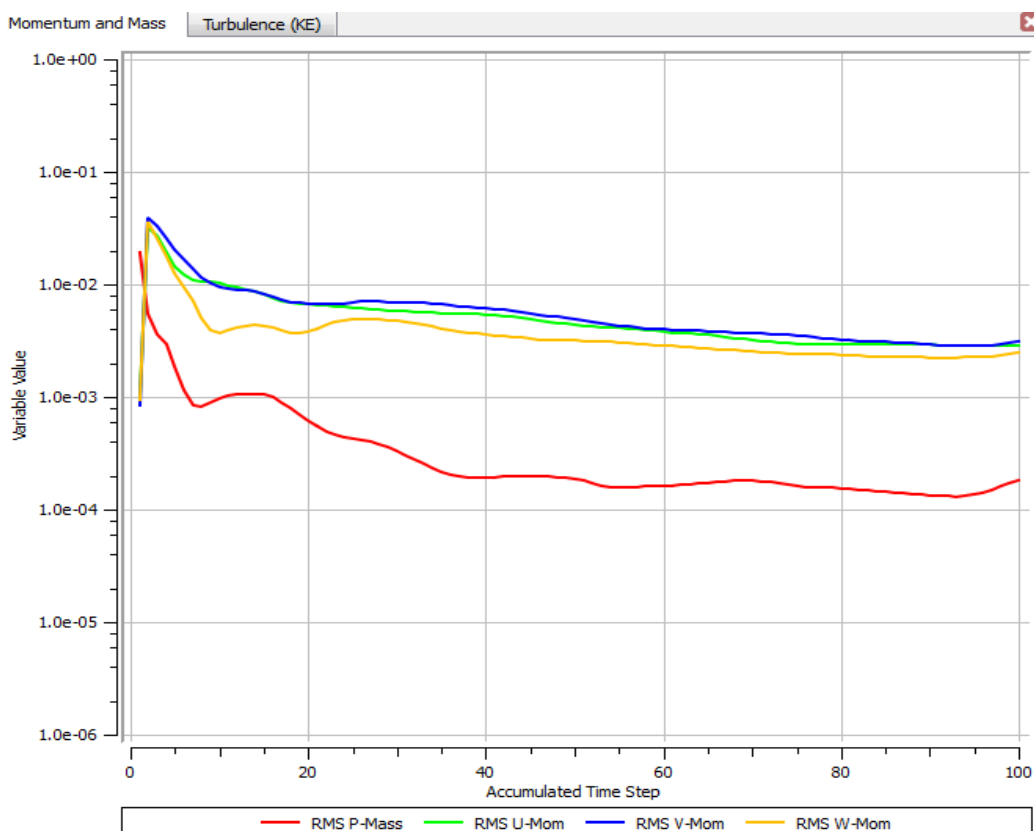


Figure 18. Residue in mass conservation equations

In the case of turbulence, figure 19 shows that the iterations stabilize around 40 iterations. Due to the stability of the residuals, the convergence criterion and the number of iterations were appropriate.

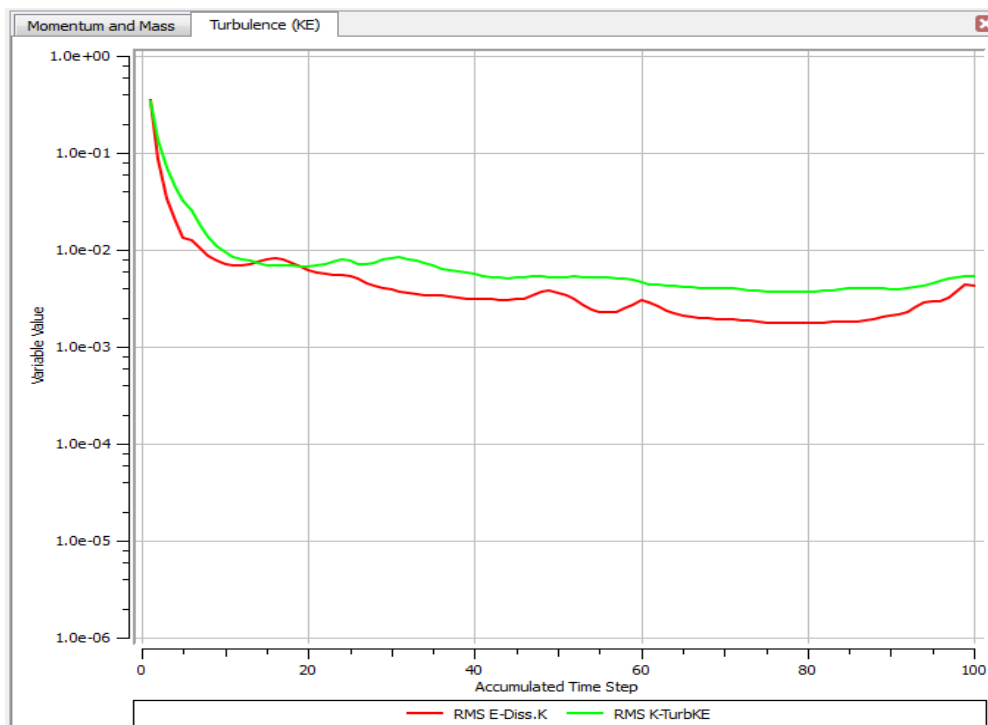


Figure 19. Residue in turbulence equations

## DISCUSSION

### Analysis of design results

Figure 20 shows that as the impeller was shortened or the pump intake was enlarged, which is the same thing happened: The pressure value at the intake gradually increases, the increase in pressure in the critical zone, the admission causes the risk of cavitation to decrease, but in exchange, the performance of the centrifugal pump decreases, as seen in figure 21. These results coincide enough to be considered stable and reliable, validating the CFD method, as mentioned by Ramirez.<sup>(33)</sup>

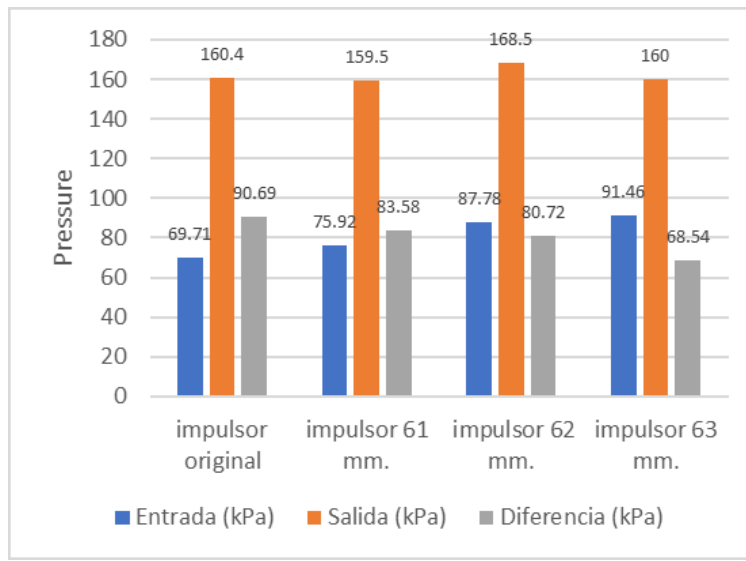


Figure 20. Comparison of pressures between different proposals

The original impeller is under absolute pressure at the inlet and outlet. Comparing the performance result of the original design obtained through CFD against the result obtained by the analytical method, it was found that there is a difference; this is because the CFD method analyzes only the centrifugal pump while the experimental method, which is the source of data for The analytical method contemplates the complete installation, which undoubtedly adds losses that are relevant to take into account.<sup>(17)</sup>

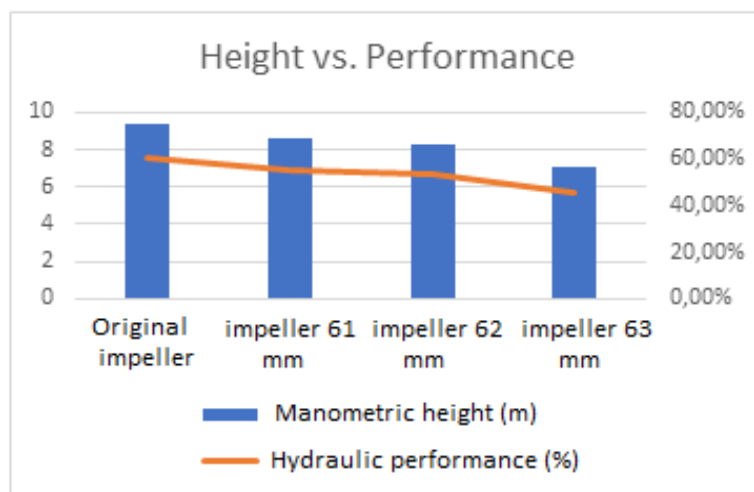


Figure 21. Redesign proposals between the comparison of heights and performances

Under normal operating conditions at 85 °C coolant temperature, water boils at a total pressure of 53830 Pa. According to the results of figure 20, cavitation will occur in none of the simulated options since the pressure values in each case are higher. However, the most critical pressure point at the pump inlet occurs at the moment of engine acceleration, so this pressure peak is evaluated below for the design proposals.<sup>(18)</sup>

Figure 22 shows that the geometric changes produce the expected changes. The analysis under normal operating conditions the intake pressure rises linearly as the intake diameter increases. This work coincides with Orlandi et al.<sup>(28)</sup>, which reports that the inlet pressure factor affects all types of pumps due to their structure and peculiar shapes.

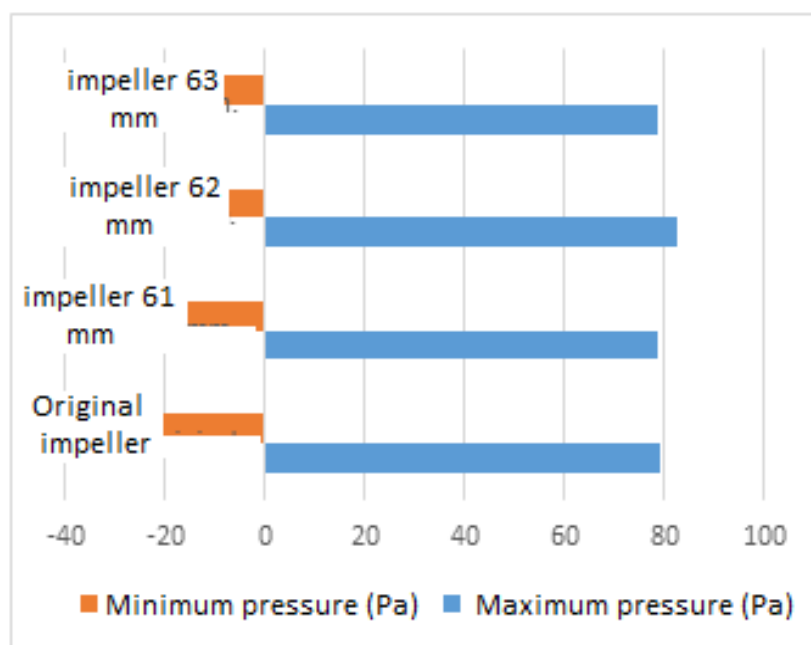


Figure 22. Pressures in sudden acceleration

The critical point in the cavitation issue occurs at the pump's inlet due to the lower pressure in that area. In order to find the most appropriate solution, several possible designs have been evaluated, in which the impeller has basically been modified. The different variables involved have been technically analyzed to consider the best option.<sup>(23)</sup>

Among the three options studied, the pump whose intake has been widened to 63 mm is the safest option to avoid cavitation. However, it is the pump with the most remarkable performance loss, with a performance drop of almost 15 % concerning the original design, which could cause problems in the cooling system.

Under normal operating conditions, the pump option with an inlet enlarged to 61 mm does not present a risk of cavitation. According to the pressure reference values during acceleration, it has also been seen that

it has a 5 % improvement compared to the original design. In terms of hydraulic performance, it is the option that represents the least loss, with 55,65 % compared to the 60,34 % performance of the original design. Taking those arguments into account, it was finally decided to choose the pump design with an impeller inlet of 61 mm; through CFD methods, it has been confirmed that it will reduce cavitation conditions.

## CONCLUSIONS

The improvement of the shape of the impeller to reduce cavitation was noted in the findings of this research, which has shown that altering the shape of the impeller in the centrifugal pump, primarily by increasing the inlet diameter, effectively reduces critical situations of low-pressure at the pump inlet. That helps reduce the likelihood of cavitation and supports using CFD simulations as an effective tool to anticipate and improve hydraulic performance in vehicle cooling systems. This progress addresses a significant gap in pump design by jointly addressing operational effectiveness and structural issues under varying operating conditions.

Concerning the experimental and numerical validation of fluid dynamics, it presents the convergence between the experimental results and those that come from CFD simulations, validating the effectiveness of the numerical models as a faithful reflection of the physical phenomena in centrifugal pumps. This combined strategy has facilitated the precise identification of critical pressure and velocity zones, providing a better understanding of turbulent flow dynamics in automotive cooling systems.

Analyzing the effect of the improved design on overall system performance, the results have shown that the suggested design changes, while helpful in reducing cavitation, involve sacrifices in water flow efficiency. However, the design that includes an enlarged inlet diameter of 61 mm presents itself as a balanced option, achieving a 5 % increase in critical pressure without a noticeable reduction in overall performance. This addresses a significant technical challenge in the sector, balancing cavitation reduction and operational efficiency.

## BIBLIOGRAPHIC REFERENCES

1. Kawamoto R, Mochizuki H, Moriguchi Y, Nakano T, Motohashi M, Sakai Y, *et al*. Estimation of CO<sub>2</sub> emissions of internal combustion engine vehicle and battery electric vehicle using LCA. *Sustainability*. 2019; 11(9):2690.
2. Kalghatgi G. Development of Fuel/Engine Systems—The Way Forward to Sustainable Transport. *Engineering*. 2019; 5(3):510-518.
3. Rocha-Hoyos JC, Tipanluisa LE, Zambrano VD, Portilla ÁA. Estudio de un motor a gasolina en condiciones de altura con mezclas de aditivo orgánico en el combustible. *Inf Tecnol*. 2018; 29(5):325-334.
4. Lü X, Wu Y, Lian J, Zhang Y, Chen C, Wang P, *et al*. Energy management of hybrid electric vehicles: A review of energy optimization of fuel cell hybrid power system based on genetic algorithm. *Energy Convers Manag*. 2020; 205:112474.
5. Broatch A, Olmeda P, Martín J, Dreif A. Improvement in engine thermal management by changing coolant and oil mass. *Appl Therm Eng*. 2022; 212:118513.
6. Llanes-Cedeño EA, Grefa Shiguango SF, Molina-Osejos JV, Rocha-Hoyos JC. Incidence of automotive air conditioning on the index of fuel consumption in spark ignition vehicle on a route in the Ecuadorian Amazon. *Ingenius Rev Cienc Tecnol*. 2024; 31:115-126.
7. Yu J, Zhang T, Qian J. Efficiency testing methods for centrifugal pumps. In: *Electr Motor Prod*. 2011. p. 125-172.
8. Puma-Benavides DS, Cevallos-Carvajal AS, Masaquiza-Yanzapanta AG, Quinga-Morales MI, Moreno-Pallares RR, Usca-Gomez HG, *et al*. Comparative analysis of energy consumption between electric vehicles and combustion engine vehicles in high-altitude urban traffic. *World Electr Veh J*. 2024;15(8).
9. Mentzos M, Filios A, Margaris P, Papanikas D. CFD predictions of flow through a centrifugal pump impeller. In: *Proc Int Conf Experiments/Process/System Modelling/Simulation/Optimization*. Athens; 2005. p. 1-8.
10. Hedi L, Hatem K, Ridha Z. Numerical flow simulation in a centrifugal pump. In: *Int Renew Energy Congr*. 2010:300-304.
11. Bacharoudis EC, Filios AE, Mentzos MD, Margaris DP. Parametric study of a centrifugal pump impeller by varying the outlet blade angle. *Open Mech Eng J*. 2008;2(1).

12. Shah SR, Jain SV, Patel RN, Lakhera VJ. CFD for centrifugal pumps: A review of the state-of-the-art. *Procedia Eng.* 2013; 51:715-720.
13. Fatigati F, Di Battista D, Cipollone R. Design improvement of volumetric pump for engine cooling in the transportation sector. *Energy.* 2021; 231:120936.
14. Derakhshan S, Pourmahdavi M, Abdolahnejad E, Reihani A, Ojaghi A. Numerical shape optimization of a centrifugal pump impeller using artificial bee colony algorithm. *Comput Fluids.* 2013; 81:145-151.
15. Wang W, Yuan S, Pei J, Zhang J. Optimization of the diffuser in a centrifugal pump by combining response surface method with multi-island genetic algorithm. *Proc Inst Mech Eng Part E J Process Mech Eng.* 2017;231(2):191-201.
16. Xu Y, Tan L, Cao S, Qu W. Multiparameter and multiobjective optimization design of centrifugal pump based on orthogonal method. *Proc Inst Mech Eng Part C J Mech Eng Sci.* 2017;231(14):2569-2579.
17. Fracassi A, De Donno R, Ghidoni A, Congedo PM. Shape optimization and uncertainty assessment of a centrifugal pump. *Eng Optim.* 2022;54(2):200-217.
18. Ramakrishna R, Hemalatha S, Rao DS. Analysis and performance of centrifugal pump impeller. *Mater Today Proc.* 2022; 50:2467-2473.
19. Giuffre A, Colonna P, Pini M. The effect of size and working fluid on the multi-objective design of high-speed centrifugal compressors. *Int J Refrig.* 2022; 143:43-56.
20. Mott NF. A theory of the fragmentation of shells and bombs. In: *Fragmentation of Rings and Shells.* 2006. p. 243-294.
21. Zhang YL, Zhu ZC, Dou HS, Cui BL. A generalized Euler equation to predict theoretical head of turbomachinery. *Int J Fluid Mech Res.* 2015;42(1).
22. Mataix C. *Mecánica de fluidos y máquinas hidráulicas.* 2<sup>a</sup> ed. Madrid: Ediciones del Castillo SA; 1986.
23. Hongyu G, Wei J, Yuchuan W, Hui T, Ting L, Diyi C. Numerical simulation and experimental investigation on the influence of the clocking effect on the hydraulic performance of the centrifugal pump as turbine. *Renew Energy.* 2021; 168:21-30.
24. Çengel YA, Cimbala JM. *Introduction to computational fluid dynamics.* In: *Fluid Mechanics: Fundamentals and Applications.* 2006.
25. Xamán, J. *Dinámica de fluidos computacional para ingenieros.* Palibrio, 2016.
26. Fernandes del Pozo D, Liné A, Van Geem KM, Le Men C, Nopens I. Hydrodynamic analysis of an axial impeller in a non-Newtonian fluid through particle image velocimetry. *AIChE J.* 2020;66(6): e16939.
27. Karlsen-Davies N-HD. Computational and experimental analysis of the effects of manufacturing tolerances on the performance of a regenerative liquid ring pump [dissertation]. Lancaster University (United Kingdom); 2017.
28. Orlandi F, Montorsi L, Milani M. Cavitation analysis through CFD in industrial pumps: A review. *Int J Thermofluids.* 2023; 20:100506.
29. Hermogenes GIL. *Manual CEAC del automóvil.* Grupo Editorial; 2003.
30. Kirchhofer M, Krieger M, Hofer D. A comparative study on numerical flow simulations of a centrifugal electronic cooling fan using four different turbulence models. *Energies.* 2023;16(23):7864.
31. Feudjio Nguefack MC, Mtopi Fotso BE, Fogue M. Optimization of the position of Savonius turbines mounted on a hybrid vehicle by CFD analysis. *Int J Green Energy.* 2022; 19(7):757-774.

32. Montalvo L. Análisis y optimización en el diseño mediante CFD de la bomba centrífuga del sistema de refrigeración del motor Kubota V3307, para fabricación nacional del elemento. 2017. <https://repositorio.uisek.edu.ec/handle/123456789/2652>
33. Ramirez R, Avila E, Lopez L, Bula A, Forero JD. CFD characterization and optimization of the cavitation phenomenon in dredging centrifugal pumps. *Alexandria Eng J.* 2020; 59(1):291-309.
34. Shrestha S, Bijukchhe PL, Chitrakar S, Thapa B, Qian Z, Guo Z. Comparative study of different erosion models in Francis runner blade using OpenFOAM. *IOP Conf Ser Mater Sci Eng.* 2024; 1314(1):012009.

#### **FINANCING**

The authors did not receive financing for the development of this research.

#### **CONFLICT OF INTEREST**

The authors declare that there is no conflict of interest.

#### **AUTHORSHIP CONTRIBUTION**

*Conceptualization:* Edilberto Antonio Llanes Cedeño, Édison Argüello Maya.

*Data curation:* Rodrigo Rigoberto Moreno Pallares.

*Formal analysis:* Juan Carlos Quinchuela Paucar.

*Research:* Lenin Montalvo Ochoa.

*Methodology:* Édison Argüello Maya.

*Project administration:* Juan Carlos Quinchuela Paucar.

*Resources:* Lenin Montalvo Ochoa.

*Software:* Lenin Montalvo Ochoa.

*Supervision:* Edilberto Antonio Llanes Cedeño, Édison Argüello Maya.

*Validation:* Rodrigo Rigoberto Moreno Pallares.

*Visualization:* Rodrigo Rigoberto Moreno Pallares.

*Writing - original draft:* Edilberto Antonio Llanes Cedeño.

*Writing - review and editing:* Edilberto Antonio Llanes Cedeño.